Atmos. Meas. Tech. Discuss., 8, 11817–11852, 2015
www.atmos-meas-tech-discuss.net/8/11817/2015/
doi:10.5194/amtd-8-11817-2015

Atmospheric Measurement Techniques
Discussions
Open Access

This discussion paper is/has been under review for the journal Atmospheric Measurement Techniques (AMT). Please refer to the corresponding final paper in AMT if available.

Retrieving clear-air turbulence information from regular commercial aircraft using Mode-S and ADS-B broadcast

J. M. Kopeć[1,2], K. Kwiatkowski[1,4,5], S. de Haan[3], and S. P. Malinowski[2]

[1]Interdisciplinary Centre for Mathematical and Computational Modelling, University of Warsaw, Warsaw, Poland
[2]Institute of Geophysics, Faculty of Physics, University of Warsaw, Warsaw, Poland
[3]Royal Netherlands Meteorlogical Institute, De Bilt, the Netherlands
[4]Institute of Theoretical Physics, Faculty of Physics, University of Warsaw, Warsaw, Poland
[5]University Centre for Environmental Studies and Sustainable Development, University of Warsaw, Warsaw, Poland

Received: 1 October 2015 – Accepted: 19 October 2015 – Published: 16 November 2015

Correspondence to: J. M. Kopeć (jkopec@icm.edu.pl)

Published by Copernicus Publications on behalf of the European Geosciences Union.

Abstract

Navigational information broadcast by commercial aircraft in the form of Mode-S and ADS-B messages can be considered a new and valid source of upper air turbulence measurements. A set of three processing methods is proposed and analysed using a quality record of turbulence encounters made by a research aircraft.

The proposed methods are based on processing the vertical acceleration or the background wind into the eddy dissipation rate. All the necessary parameters are conveyed in the Mode-S/ADS-B messages. The comparison of the results of application of the processing against a reference eddy dissipation rate obtained using on-board accelerometer indicate a significant potential of those methods. The advantages and limitation of the presented approaches are discussed.

1 Introduction

Despite emergence of new forecasting techniques and availability of better forecasts the encounters of turbulence are the main cause of aviation incidents among commercial aircraft in the cruise phase (NTSB, 2011, 2012). The lack of on-board detectors that could provide appropriate warning for the pilot forces airmen to rely solely on forecasts or any slight visual characterizations (e.g. bands in cirrus Trier et al., 2010) of the presence of this otherwise invisible phenomenon. Yet the scales of turbulence "detected" by the aircraft cause significant problems in forecasting. Most commercial aircrafts are susceptible to turbulence on scales from 10 m up to 1 km (Lester, 1994). This is still below scale range modelled by the numerical weather prediction (NWP) models whose spatial resolution is in range from 1.5 up to 30 km. Some trials have been made to use sub-grid scale schemes of NWP models for direct estimation of turbulence (Trier et al., 2012). However, in order to give reasonable results, such approach requires resolutions higher than current operational standard. As of now most operationally used forecasting techniques infer clear-air turbulence (CAT) behaviour from larger scales resolved in the NWP models (e.g. Sharman et al., 2006; Gill and Buchanan, 2014). This methodology is based on widely accepted assumption that due to the turbulent energy cascade the presence of resolved scale turbulence is implying the presence of sub-scale turbulence. However, NWP based forecast is bound to generate errors and requires sophisticated statistical corrections (Williams, 2014; Sharman et al., 2006; Kim et al., 2015).

Aside from forecasting, CAT poses a broad field of research (Sharman et al., 2012) as its presence is determined by complex mechanisms accompanying hydrodynamical instabilities. The basic generation mechanisms include buoyancy waves breaking, flow over complex topography, presence of deep convection and significant wind shears with Kelvin–Helmholtz instabilities. All of those mechanisms are responsible for the presence of turbulence in the upper troposphere that is hardly visible, except for the cases where the flow disturbs nearby cirrus clouds. At the same time it is impossible to detect it using ordinary weather radars. The only feasible remote detection method is by using active optical sensing (Vrancken, 2015). On board devices allowing this are now in very early stages of development. Presently the most accurate method of measuring CAT is a dedicated airborne experiment (Koch et al., 2005; Veerman et al., 2014). However in order to gain satisfactory information about such a complex phenomenon a large number of those expensive, time-consuming experiments would be required. Other sources of information are the standard turbulence reports provided by the commercial aircraft (PIREP, AMDAR/ACARS). For a long time investigation of kilometre scale turbulence dynamics based on those reports was limited due to their sparse spatial resolution. The situation changed with introduction of in situ eddy dissipation rate (ϵ; notation used: EDR = $\epsilon^{\frac{1}{3}}$) measurements (Cornman et al., 1995) with reporting resolution of order of 10 km. The new resolution allowed for in-depth investigation of near cloud turbulence and new insight into its occurrence (Trier et al., 2010; Trier and Sharman, 2009). The only drawback of the EDR data is that it still is not an industry standard, hence its availability is an effect of negotiations with the individual airlines. This in turn severely limits the extent and volume of the available data.

AMTD
8, 11817–11852, 2015

In the present paper we propose a new method of gaining information about turbulence from regular commercial aircraft and demonstrate its viability. The proposed method is based on a non-standard source, namely the Mode-S EHS (Enhanced Surveillance) data. The Mode-S is a part of secondary surveillance radar (SSR) – a system supporting air traffic management (ATM) – and to our best knowledge it was not considered a source of turbulence measurements previously. Mode-S is a protocol of information exchange between the aircraft and the ATM system. It is based on exchange of short status messages or requests. The messages that are an integral part of the Mode-S are exchanged with a very high sampling rate ranging from 0.2 up to 2 Hz (ICAO, 2007a, 2004) on frequencies 1090 and 1030 MHz. The messages are not encrypted and thus can be received and decoded by a relatively simple hardware (Haan et al., 2013). It has been shown (Haan, 2011) that the Mode-S carries a very high frequency wind information. The methods we propose use this high frequency measurements and the position information in order to gather turbulence measurements with spatial resolution of approximately 25 km which is comparable to the in situ EDR data. We also propose a method to extract turbulence information from a class of navigational messages named automatic dependent surveillance-broadcast (ADS-B). ADS-B are 1090 MHz band messages spontaneously transmitted by the aircraft and formatted in the manner similar to the Mode-S. The ADS-B messages do not contain wind information and are broadcast with sampling rate between 1 and 6 Hz. The potential advantage of proposed methods over the in situ EDR is the significantly larger volume of available information since very significant part of civil aviation aircraft worldwide use the Mode-S protocol. Especially taking into account the fact that the setting up of Mode-S/ADS-B receiving station requires relatively low amount of work and is relatively cheap.

AMTD
8, 11817–11852, 2015

2 Data used for analysis

2.1 Dataset details

It is hard to find a turbulence encounter for which both a good scientific-grade recording and the archive of the Mode-S data are available at a same time. We managed to identify a record of Mode-S messages broadcast by a research aircraft during a flight campaign targeted explicitly at CAT measurements (Veerman et al., 2014). The Mode-S record was received and stored by the Royal Dutch Meteorological Institute (KNMI). The KNMI data were collected using a locally installed receiver with spatial range marked in Fig. 1. Due to this limitation there is no overlapping record of turbulence encounter but there are numerous overlapping flight fragments allowing for proper analysis based on the flight campaign dataset processed into Mode-S-like form. This processing can be defined and verified using the overlapping flight fragments.

The KNMI dataset comprises of mixed ADS-B and Mode-S EHS messages. For details on a way the messages are captured, interpreted, processed and stored see Haan et al. (2013). The available overlapping data are characterized by varying level of quality and availability. Summary of the KNMI data content can be found in Table 1. For a technical reason part of Mode-S EHS messages containing the track angle parameter of the research aircraft were missing from KNMI archive.

Since the KNMI data lack turbulence encounters and some essential parameters (low availability of velocities and lack of track angle) the analyses conducted in this paper are mainly based on a dataset originating from flight measurement campaign conducted as a part of EU 7th Framework Programme project DEmonstration of LIdar based Clear-Air Turbulence detection (DELICAT) (Veerman et al., 2014). The campaign was aimed at testing the feasibility of using a forward looking lidar system as an early warning turbulence detector which was the main aim of the DELICAT project itself. The aircraft used for flight tests was a modified Cessna 550 Citation II aircraft belonging to National Aerospace Laboratory, Netherlands (NLR). The aircraft was equipped with the mentioned forward looking lidar system, nose boom for side-slip and angle of attack

AMTD
8, 11817–11852, 2015

measurements, Inertial Reference System (IRS) equipped with a 3-D accelerometer and Digital Air Data Computer (DADC). Eleven flights were conducted in the period between 17 July and 13 August 2013. The data types and sources used for the analyses presented later are listed in Table 2.

For further analysis we have chosen three flights designated as FL6, FL8 and FL9. Flight FL6 was conducted on 6 August 2013 while the two remaining flights have taken place on 8 August 2013. Flights FL6 and FL8 were first of all selected because they overlap with relatively long Mode-S/ADS-B records by KNMI. No turbulence was encountered during those flights. However turbulence was reported by other aircraft in the vicinity during FL8. Flight FL9 was selected because of multiple CAT encounters of light to borderline moderate (peak vertical acceleration 0.4 g) intensity as shown in Figs. 1 and 2. Therefore the analysis will be based on three very different flights: turbulent flight (FL9) for validity check, calm flight for (FL6) sanity check and calm flight with turbulence reported in vicinity (FL8) for detection precision check. The reference EDR has been calculated according to the method outlined in (WMO, 2003) based on the high-frequency reading of the on-board accelerometer.

2.2 Dataset discussion

In order to evaluate the appropriateness of the methods proposed in this paper we need to apply them to the Mode-S data covering some turbulence encounters. Unfortunately no record of the original Mode-S transmissions of the research aircraft was preserved that would include any turbulence encounter. Therefore we processed the high-quality record of the DELICAT flight parameters of the aircraft in order to obtain an output that is intended to mimic the data sent by the Mode-S transponder. This processing was performed taking into account the technical parameters of the Mode-S protocol (including data sources, resolution, sampling rate, etc.) outlined in (ICAO, 2007a, 2004; Grappel and Wiken, 2007). The original Mode-S data recorded by KNMI were then used as a reference for evaluating the successfulness of the processing on the overlapping flight fragments.

AMTD
8, 11817–11852, 2015

The processing allowing for the DELICAT data to mimic the transponder output occurred to be quite simple:

1. Choice of the sampling rate. For the reference KNMI data the sampling rate was on average 1.5 Hz for flight 9 and 1.25 Hz for flight 8 due to data loss on reception. However, when the largest (few second) gaps are discarded the average sampling rate for both cases goes up to approximately 2 Hz. This number was chosen for preparation of the ADS-B imitation For Mode-S imitation we have chosen 0.25 Hz which corresponds to the typical rotation speed of the SSR ATC radar antennas (ICAO, 2007b).

2. The data contained in one sampling period are averaged. The averaged data are then discretized to match the reference data resolution summarised in Table 1. Discretization is performed using simple floor function.

The resulting data can be divided into 3 groups:

1. Very good agreement between the reference and processed data as it is presented in Fig. 3. The DELICAT data originate from the DADC which is also the source for the Mode-S transponder.

2. Very good agreement but data is shifted by some nearly constant bias. This is valid for: 2-D position (approximately 2 km horizontal shift as shown in Fig. 4) and heading (approximately 2° bias). Those differences are small and almost constant thus not distorting the results in any significant way. Data were accepted as correct.

3. Large shift in data noticeably changing over time: air speed and ground speed (both biased by 25 $\mathrm{m\,s^{-1}}$). This is despite the fact that the data source was the same.

First two groups indicate that the processing algorithm is satisfactory. Even though it occurred that 2-D position (longitude and latitude) reported in the DELICAT research

AMTD
8, 11817–11852, 2015
Clear-air turbulence information from regular commercial aircraft
J. M. Kopeć et al.

data is not as accurate as that reported in the ADS-B/Mode-S. However the existence of third group might be bothersome. We have cross-checked the consistency of the ground speed record with the reported changes in the geographical position of the aircraft reported both in the KNMI and the DELICAT data. Although such estimate introduces additional errors it was clear that the ground speed recorded in KNMI was inconsistent with any of the three other ground speed estimates as it is presented in Fig. 5 (for the case of FL8). This inconsistency and the fact that velocities were reported in a very small fraction of data and in short interrupted periods indicate a possibility of systematic errors in reception.

In the case of altitude we have discovered that in ascent/descent phases of flight the data received by the KNMI agree less with the DELICAT data than in the cruise phase (usually altitudes exceeding 7.5 km), but these errors were relatively small. It was approximately 3–18 m when vertical velocity was high and dropping to less than 6 m at the cruise altitudes when the flight was stable. Moreover the error dominant sign was dependent on whether the aircraft was descending or ascending (negative for descend as shown in Fig. 3) which rather suggests existence of a small time lag between the DELICAT and KNMI records rather than necessarily error of this magnitude.

In summary the reference data collected by the KNMI receiver proved to be insufficient for conducting tests of the post-processing methods. This is mainly due to lack of track angle record and poor quality of existing speed records. To mitigate this we have established a method of processing the DELICAT data into Mode-S/ADS-B form. The output of this processing was verified against the reference KNMI data and deemed satisfactory.

3 CAT estimation algorithms

In the following section we propose three methods processing the Mode-S and ADS-B data into potentially useful information. The first of those methods uses only the data available in ADS-B spontaneous transmissions which guarantees independence from

AMTD
8, 11817–11852, 2015

Clear-air turbulence information from regular commercial aircraft

J. M. Kopeć et al.

the presence of the ground based interrogators. This increases the reception coverage significantly. The second and third methods require more information and hence full set of Mode-S EHS data.

3.1 Method 1: vertical acceleration

The usual indicator of CAT encounter is the magnitude of the vertical acceleration of the aircraft. This is what effectively the passengers feel and what is reported in the simplest AMDAR messages containing the so-called Index of Turbulence (IT). However, the value of the peak acceleration as measured by the aircraft poorly reflects the state of the background atmosphere (WMO, 2003). This is mainly due to the fact that various aircraft are characterized by vastly different aerodynamic properties which leads to large variation in response to the vertical gusts characteristics. Moreover neither Mode-S nor ADS-B contain information about acceleration itself. Yet they both carry altitude and vertical velocity information and in case of ADS-B transmissions the reporting frequency is between 0.5 and 1 Hz. Using this information the vertical acceleration of the aircraft can be calculated using the simple formulas:

$$\frac{dz}{dt} = v_z \tag{1}$$

$$\frac{dv_z}{dt} = a_z \tag{2}$$

Here z is the altitude, v_z is the vertical velocity and a_z is the vertical acceleration. The time derivative is approximated simply as finite difference between the consecutive observations. The a_z obtained in this way is then processed as described in (WMO, 2003) in order to obtain the EDR estimate. This method employs a simple formula which models the aircraft response to the homogeneous, isotropic turbulence spectrum.

$$\epsilon = B\sigma_T^3 V^{-1} \tag{3}$$

Discussion Paper | Discussion Paper | Discussion Paper | Discussion Paper |
AMTD
8, 11817–11852, 2015
Clear-air turbulence information from regular commercial aircraft
J. M. Kopeć et al.

Here B is an adjustable constant accounting for the unknown responsiveness factor of the aircraft, σ_T is the standard deviation of acceleration measurements in a set period of time T and V is the true air speed (TAS) of the aircraft.

Another way to salvage the same formulas (Eqs. 1–3) is to use the inertial vertical velocity (IVV) information which is present in the ADS-B. It also has quite coarse resolution of 32 ft min^{-1} (0.16 m s^{-1}). The potential advantage is that since we start with an estimate of vertical velocity we can use first order finite differences to get an estimate of the vertical acceleration. In Sects. 4 and 5 we present and discuss results from both approaches: IVV and altitude derived EDR. We will call them IVV EDR and ALT EDR respectively.

Although this CAT estimation method is based solely on ADS-B which extends the coverage it has a number of drawbacks. First of all the ADS-B data do not contain TAS therefore there are three possible ways to use the above formula:

- Combine the information from Mode-S EHS about the true air speed (TAS) with high resolution altitude and vertical rate. In this way however we lose the advantage of territorial coverage.

- Assume constant TAS (which is not a particularly good approximation) and use only ADS-B.

- A third option would be to use an external wind information from for example NWP model and use this to recalculate TAS from the ground track. It will introduce an uncertainty related to the external wind source. This option will not be discussed here.

Another factor lowering effectiveness of this method is reporting resolution of the altitude in the ADS-B which is 25 ft (7.62 m). This causes the acceleration signal based on such an altitude profile to be erroneous and unrealistic. In order to mitigate this, prior to processing we have applied a second order Butterworth band-pass filter with limiting frequencies 0.025 and 0.050 Hz. Assuming that an typical commercial jet aircraft is cruising at 250 m s^{-1} these frequencies corresponding to the spatial scales of

10 and 5 km respectively. The scale range below 5 km occurred to be dominated by the quantization noise. Analogous filtering was applied to IVV data.

Finally there is one more potential issue that this method may display that will not be visible in the present paper since all data presented here are derived from only one aircraft. Equation (3) is an approximation since in WMO (2003) B incorporates the aircraft response integral which may have very diverse values for various aircraft types. Basically this integral depends on some basic aircraft characteristics (wing area, mass, lift, etc.) and the flight conditions (TAS, the air density) (Wright and Cooper, 2014). Treating B as a constant means holding the aircraft type, TAS and air density as constant too. This will require very cautious use when applying to the data derived from the aircraft of varying type.

3.2 Method 2: the structure functions

The second proposed method is aimed to retrieve characteristics of the turbulence independently of the aircraft type. To achieve this goal we will employ a method of estimating structure functions value based on high frequency wind velocity measurements. The structure function estimate is obtained as follows (Frehlich and Sharman, 2010):

$$D_{\mathrm{LL}}(r) = \langle (u_{\mathrm{LL}}(\boldsymbol{x}) - u_{\mathrm{LL}}(\boldsymbol{x}+\boldsymbol{r}))^2 \rangle_{\boldsymbol{x}} \tag{4}$$

Here u_{LL} denotes the component of the horizontal wind velocity vector along the track of the aircraft, x is a position of measurement, $\boldsymbol{r}$ is the displacement vector, $r = |\boldsymbol{r}|$ is the displacement distance and $\langle \cdot \rangle_{\boldsymbol{x}}$ stands for position averaging. The position averaging in our setting will be understood as the mean of N observations performed by the same aircraft separated by a constant distance r. This is somewhat different from the averaging used in Frehlich and Sharman (2010) and Monin and Yaglom (1975). In both of those publications authors mean ensemble average as an average over many realizations of the similar conditions. However when using this methodology in post processing of individual aircraft flight record we make an assumption that a series of consecutive observations of sufficient length forms such an ensemble. This assumption

AMTD
8, 11817–11852, 2015

is based on the fact that commercial aircraft have velocity much greater than velocity perturbations associated with atmospheric turbulence at a kilometre spatial scale.

It is then assumed that the structure function estimate $D_{LL}(r)$ can be expressed as:

$$D_{LL}(r) = C\epsilon^{\frac{2}{3}} r^{\frac{2}{3}} \tag{5}$$

Here C is a constant. The theoretical value of C is close to 2 (Sreenivasan, 1995). In order to obtain ϵ one needs to combine formulas 4 and 5. This allows us to estimate the magnitude of EDR based on regressing $\log D_{LL}(r)$ against $\log r$. However in our case the separation can only take values from a discrete range determined by the intervals between the consecutive Mode-S messages broadcasting. Those values are very sparsely distributed in the range up to 10 km, where according to Frehlich and Sharman (2010) the structure function scaling is present. Typically observations are separated by approximately 0.8–1.1 km which results in 9–12 different r values for the mentioned scale range. In practice this sparsity can be even greater due to receiver loss factor. In addition to this sparse distribution the estimates of D_{LL} are impacted by effects of quantization noise in source data. This requires us to again use the second order Butterworth filter. Since in the case of wind the quantization noise is not as significant we have chosen a band better covering the expected CAT scales. The limiting frequencies were chosen to be 0.025 and 0.094 Hz which corresponds to spatial scale between 10 and 2.6 km respectively.

3.3 Method 3: threshold crossing

The last method we present is also based on high resolution wind measurements. However this time we will employ a method described in Poggi and Katul (2010). The method is based on relating a density function of threshold crossing (N_d) to the eddy dissipation rate. For a series of N consecutive measurements of longitudinal velocity component at discrete times $t_i, i \in \{1,...,N\}$ the density of threshold crossing is defined

AMTD
8, 11817–11852, 2015

as follows:

$$N_\mathrm{d}(T_c,N) = \frac{\sum_{i=0}^{N} I(t_i,T_c)}{N-1} \tag{6}$$

Here T_c is a non-dimensional threshold (positive or negative) and the indicator function $I(t_i,T_c)$ is defined as follows:

$$I(t_i,T_c) = \begin{cases} 1 & \text{if } \left[\frac{u_\mathrm{LL}(t_i)}{\sigma_u} - T_c\right]\left[\frac{u_\mathrm{LL}(t_{i+1})}{\sigma_u} - T_c\right] < 0 \\ 0 & \text{otherwise} \end{cases} \tag{7}$$

Here σ_u denotes the local root mean square of the longitudinal velocity fluctuations u_LL. Following Poggi and Katul (2010) threshold crossing density can be related to ϵ using:

$$\epsilon = \frac{15\pi^2}{2} \nu \sigma_u^2 e^{T_c^2} N_\mathrm{d}^2(T_c,N) \tag{8}$$

Here ν denotes the kinematic viscosity. For calculations in this paper we have taken ν to be the kinematic viscosity at the altitude of 11 km as defined by the U.S. Standard Atmosphere (NASA, 1976). In our setting the wind velocity estimate is first filtered before passing to the threshold crossing based estimator. The filtering serves to remove both the mesoscale tendencies and high frequency noise. For this purpose we have used again the second order Butterworth band-pass filter. The filter limiting frequencies were 0.025 and 0.094 Hz which correspond roughly to 10 and 2.6 km respectively.

3.4 Methods: summary

We consider all three methods here because of their possible varying application. The first method uses only the vertical position (or vertical velocity) information. This information is available in ADS-B frames. This makes it possible to receive this kind of data globally since ADS-B broadcast is not limited to any areas. This is in contrast to the territorial extent of Mode-S data being determined by the presence of the ground based interrogators. The main disadvantage of this method is its obvious dependence on the aircraft type. Second and third methods (structure functions and threshold-crossing) need high resolution wind measurements thus their range of application is limited to the areas where Mode-S EHS is available. These are the main disadvantages of those methods. However both of those methods are based on quite robust understanding of turbulence physics. Moreover using the background wind as a source of information should make the measurements inherently aircraft independent.

The most interesting question is whether the available time resolutions of the measurements (approximately 4 s for Mode-S and up to 0.5 s for ADS-B) will allow for the successful extraction of turbulence information.

4 Results

For each flight we have calculated a set of four EDR estimations:

1. ADS-B method based on IVV (IVV EDR);
2. ADS-B method based on altitude (ALT EDR);
3. Mode-S based structure function method;
4. Mode-S based threshold crossing method;

Results of ADS-B EDR based methods along with the reference EDR were arbitrarily normalized for appropriate presentation in Figs. 6– 8. This scaling is possible since they are determined up to a constant. On the contrary, the threshold crossing EDR (according to Eq. 8) as well as the structure function based EDR is known exactly (when assuming the theoretical value of $C = 2$ in Eq. 5).

The threshold crossing EDR estimate displays values much smaller than those measured by the standard on-board sensors. 0.05 $\mathrm{m}^{\frac{2}{3}}\mathrm{s}^{-1}$ for our estimate vs. 0.18 $\mathrm{m}^{\frac{2}{3}}\mathrm{s}^{-1}$

Discussion Paper | Discussion Paper | Discussion Paper | Discussion Paper |

AMTD

8, 11817–11852, 2015

Clear-air turbulence information from regular commercial aircraft

J. M. Kopeć et al.

Title Page
Abstract Introduction
Conclusions References
Tables Figures
◂ ▸
Back Close
Full Screen / Esc
Printer-friendly Version
Interactive Discussion

for small business jet aircraft as reported in Sharman et al. (2014). This can have various underlying causes. One of the most likely causes is the fundamental difference between the form and properties of canopy turbulence considered in (Poggi and Katul, 2010) and the upper tropospheric/lower stratospheric turbulence investigated in the current analysis. The former is considered isotropic and homogeneous in measurement scales while the latter is often non-isotropic down to scales well below Mode-S/ADS-B resolution and frequently intermittent (Cho et al., 2003). Thus the constant quantity $7.5\pi^2$ that can be found in Eq. (8) may differ significantly for our cases.

As well as the threshold crossing method the structure function based approach results in an underestimation, when using $C = 2$ in Eq. (5). The peak value of the recorded EDR in FL9 is $0.12\,\mathrm{m^{\frac{2}{3}}\,s^{-1}}$ for the borderline moderate case while the maximum value of EDR observed during light turbulence encounters was $0.09\,\mathrm{m^{\frac{2}{3}}\,s^{-1}}$. This is much closer to the PIREP based values but still too low. In order to achieve EDR consistent with the small business jet thresholds in (Sharman et al., 2014) one must reduce C to 1 which in turn is inconsistent with the fact that C is known quite robustly to be approximately 2 over a large set of various flows (Sreenivasan, 1995).

Due to the large differences in EDR estimate values for the sake of presentation in Figs. 6–8 we have also arbitrarily normalized the threshold crossing and the structure function based estimates along with the ADS-B based results. Gaps on the plots are the result of discarding some flight fragments as unreliable. An unreliable flight fragment in our understanding is related to manoeuvres – either turn or significant ascent or descent. Those events will introduce (potentially large) errors. The observation was discarded if the roll off the aircraft was exceeding 7° in the 45 s neighbourhood of the observation or the 180 s moving average absolute value of the vertical velocity was greater than $1.3\,\mathrm{m\,s^{-1}}$.

All of the methods display some potential in detecting turbulence. As indicated in Fig. 6 all of them have correctly identified the occurrence of borderline moderate clear air turbulence (MOD event) during FL9. However, except for that there are significant differences. ADS-B altitude based approach is suffering from a high level of background noise. This does not allow to identify anything besides the single MOD event in FL9 simply because the light turbulence signal is drowned in the noise. ADS-B IVV based approach has much lower noise but it displays false MOD signal in calm air during flights FL9 and FL8. While FL9 false signal can be attributed to the aircraft manoeuvres (slight turn with quite sudden loss of altitude) there is no explanation recorded in the data for FL8 issue. Wind based Mode-S methods displayed no such issues. There seems to be no significant false positive signal in any of the flights whilst all of the FL9 maxima were identified correctly by both methods. The noise levels in both cases were low enough for successful light turbulence recognition. However both wind methods are much less precise in reflecting the location of the turbulence. Methods are characterized by an error of up to 100 s in peak turbulence displacement which corresponds to approximately 25 km for the cruise speed of 250 $\mathrm{m\,s^{-1}}$.

5 Discussion of the results

We will begin our discussion with a parameter sensitivity analysis of the four analysed methods. In case of the ADS-B based methods it is clear from the Eq. (3) that there is only one free parameter – the length of period of moving variance calculation. This parameter is set to 30 s. Higher values flatten the signal too much (acting not unlike an ill gauged low pass filter) while lower cause too many spikes to arise making the signal illegible. In the reference publication (WMO, 2003) this period is set to 10 s. In our case this occurred to be too small value due to quantization noise and filtering.

In case of the structure function method there is only one parameter – the period of flight time included in the single averaging. This parameter is now set to 30 s. Lower values seem to be unreasonable (too low number of cases for averaging) while higher act as an additional low-pass filter that reduces the signal.

Threshold crossing method has three free parameters: moving variance window, non-dimensional threshold value and indicator function window. As for indicator function too small window (less than 10 s) causes stray peak signals to arise. However

AMTD
8, 11817–11852, 2015

longer time periods for indicator function do not damp the signal. Windows as big as 360 s were tested and still showed quite clear response. In the end we have settled for 60 s window. This quantity can be probably still tuned using more observations. The other parameters are much more critical for successful employment of this method. The moving variance window is again acting like a low pass filter if set to higher values. We have found out that already 35 s is too much. In our calculations this value has been set to 20 s. The most critical parameter is the non-dimensional threshold T_C. The general behaviour is as expected: the bigger the modulus of T_C the weaker the signal. However if the absolute value of T_C is too small the signal also becomes illegible. This is in accordance with observations of Poggi and Katul (2010). The disturbing feature of this method is that results for positive and negative T_C are somewhat different. For positive T_C the signal appears at 0.25 and quickly vanishes at 0.45 also the FL9 MOD event is quite weak. For negative thresholds the signal was appearing at −0.2 and disappears at −0.6 and the MOD event is more pronounced. Example of T_C sign comparison is in Fig. 9. This lack of symmetry is quite unexpected but there exist a range of absolute values of T_C where still, regardless of sign, the method allows for detection of turbulence and for the correct differentiation of its intensity.

Another question is how good is the constant TAS approximation for ADS-B based methods. DELICAT flights show up to 30 % variance of TAS during cruise phases of the flights and one can expect this to influence the results significantly. However the comparison of real TAS EDR estimates vs. constant TAS EDR estimates show that the application of real TAS did not change much in any of the studied cases (see Fig. 10 for a FL9 example). In general this could be an issue, especially for the long-haul flights. Yet in the present analysis the constant TAS approximation was satisfactory.

Another source of error can be the filtering. For the present paper we have selected the second order Butterworth filters with limiting frequencies that are as much based on physics as possible. The upper bound (10 km) was introduced based on the previous studies and knowledge of turbulence scales (Lester, 1994; Frehlich and Sharman, 2010). The lower bound was driven by the limitations resulting from the signal

AMTD

8, 11817–11852, 2015

discretization and sampling rates. Also we have used the Butterworth filter due to its relatively simple response characteristics. One can imagine a better suited filtering, however we had to few cases at our disposal to try to find such filter as over-fitting would be the likely result.

It is also worthwhile to mention potential areas of use for those methods. All of the described methods allow a potential observer to use quite cheap and simple set-up for observing upper air turbulence analogous to Haan et al. (2013) or Drüe et al. (2013). All of the methods use commercial aircraft as "sensors" so measurements in the regions not frequented by the aircraft are not feasible. Another limitation is the need for Mode-S/ADS-B transponders. In most of the highly developed regions the implementation of this technology is well under way. Most newly produced aircraft are properly equipped. However, older aircraft in less developed regions of the world can be quite useless. The potential coverage is method dependent. ADS-B methods are based on spontaneous aircraft transmissions thus allowing for potentially global reception. Mode-S, however are limited to the areas with the SSR Mode-S coverage which is in turn limited by the presence of the dedicated ground based installations.

In the end one must also consider that both of the ADS-B methods are heavily aircraft dependent which is not visible in the analysis based on a single aircraft measurements while Mode-S methods dependence on aircraft type should be limited since both Mode-S methods are wind based.

6 Conclusions

We have proposed and made initial feasibility analysis of a set of four approaches aiming at measuring the turbulence using the commercial aircraft with help of the Mode-S and ADS-B protocols. Based on the available comparative material all of the methods have been found to have some potential for finding turbulence. In the scope of our study ADS-B methods were performing much worse than the Mode-S methods. The former were allowing only for a reliable recognition of a single FL9 borderline moderate case

Discussion Paper | Discussion Paper | Discussion Paper | Discussion Paper |

AMTD

8, 11817–11852, 2015

Clear-air turbulence information from regular commercial aircraft

J. M. Kopeć et al.

while the latter were allowing for quite faithful recreation of the turbulence presence and for differentiation into light and moderate categories.

Of the ADS-B methods the IVV based calculation was better but we found that it is prone to display a very strong false signals which would disqualify this method as a reliable source of measurements. In contrast both of the Mode-S methods were performing almost flawlessly. We have compared the well-known structure function approach with a threshold-crossing method that, to our best knowledge, has not been used in analysing upper air data so far. Of those two the threshold-crossing method requires more parameter fine tuning, yet the final performance of both methods was very similar.

Since the analysis presented here is only a feasibility check it is necessary to conduct further research employing a systematic comparison of the Mode-S/ADS-B records against a reliable and proven source of turbulence measurements. For this purpose the in situ EDR data Cornman et al. (1995) seem very appropriate. One just needs to identify a region where Mode-S/ADS-B transmissions of an EDR broadcasting aircraft can be recorded and stored systematically. We are planning to run such validation over the Maastricht Upper Area Control Centre (MUAC) airspace sector in near future.

Also a great advantage of Mode-S/ADS-B based measurements is the ease, simplicity and low price of the measurement set necessary to cover quite significant areas. One could even imagine that networks of such cheap receivers can be established. Another option is close cooperation with air navigation service providers who receive and store Mode-S and ADS-B. Yet another way of establishing observation network is cooperation with the existing communities such as e. g. flightradar24.com.

Data availability

The data used in this paper can be found in two sources. The reference Mode-S/ADS-B data was supplied by the KNMI. Use and distribution of this data is restricted by the appropriate KNMI policies. Access to this data can be granted by KNMI. The data collected by the DELICAT research aircraft can be accessed through the NLR. Use and distribution of this data is restricted by the appropriate NLR policies and the DELICAT

AMTD
8, 11817–11852, 2015

grant agreement. Neither dataset is currently publicly available due to the aforementioned restrictions.

Acknowledgements. The data collected during the DELICAT campaign which has received funding from the Seventh Research Framework Programme of the European Union (FP7/2007-2013) under grant agreement no. 233801. The data was collected by NLR, the Netherlands. Jacek M. Kopeć's research is financed by National Science Centre, decision no. DEC-2013/11/N/ST10/00756. Jacek Kopeć would like to thank members of the DELICAT consortium (especially P. Vrancken and H. Veerman) for their helpful remarks on this paper.

References

Cho, J. Y. N., Newell, R. E., Anderson, B. E., Barrick, J. D. W., and Thornhill, K. L.: Characterizations of tropospheric turbulence and stability layers from aircraft observations, J. Geophys. Res., 108, 8784, doi:10.1029/2002JD002820, 2003. 11831

Cornman, L. B., Morse, C. S., and Cunning, G.: Real-time estimation of atmospheric turbulence severity from in-situ aircraft measurements, J. Aircraft, 32, 171–177, doi:10.2514/3.46697, 1995. 11819, 11835

Drüe, C., Deimel, S., and Hoff, A.: A low-cost approach to derive upper-air wind measurements from ADS-B, in: 13th EMS Annual Meeting, Reading, 9–13 September 2013, available at: http://presentations.copernicus.org/EMS2013-702_presentation.pdf (last access: 21 August 2015), 2013. 11834

Frehlich, R. and Sharman, R.: Climatology of velocity and tempera-ture turbulence statistics determined from rawinsonde and ACARS/AMDAR data, J. Appl. Meteorol. Clim., 49, 1149–1169, doi:10.1175/2010JAMC2196.1, 2010. 11827, 11828, 11833

Gill, P. G. and Buchanan, P.: An ensemble based turbulence forecasting system, Meteorol. Appl., 21, 12–19, doi:10.1002/met.1373, 2014. 11819

Grappel, R. D. and Wiken, R. T.: Guidance Material for Mode S-Specific Protocol Application Avionics, Tech. Rep. ATC-334, Lincoln Laboratory, MIT, Lexington, MA, USA, available at: https://www.ll.mit.edu/mission/aviation/publications/publication-files/atc-reports/Grappel_2007_ATC-334_WW-15318.pdf (last access: 7 August 2015), 2007. 11822

AMTD

8, 11817–11852, 2015

Clear-air turbulence information from regular commercial aircraft

J. M. Kopeć et al.

Haan, S.: High-resolution wind and temperature observations from aircraft tracked by Mode-S air traffic control radar, J. Geophys. Res., 116, D10111, doi:10.1029/2010JD015264, 2011. 11820

Haan, S., Haij, M., and Sondij, J.: The use of a commercial ADS-B receiver to derive upper air wind and temperature observations from Mode-S EHS information in the Netherlands, Tech. Rep. TR-336, KNMI, De Bilt, The Netherlands, available at: http://www.knmi.nl/bibliotheek/knmipubTR/TR336.pdf (last access: 6 August 2015), 2013. 11820, 11821, 11834

ICAO: Manual on Mode S Specific Services, Montreal, Canada, 2004. 11820, 11822

ICAO: Annex 10 to the Convention on International Civli Aviation: Aeronautical Communications, International Civil Aviation Organisation, Montreal, Canada, 4th edn., 2007a. 11820, 11822

ICAO: Guidance Material on Comparison of Surveillance Technologies (GMST), available at: http://www.icao.int/APAC/Documents/edocs/cns/gmst_technology.pdf (last access: 12 August 2015), 2007b. 11823

Kim, J.-H., Chan, W. N., Sridhar, B., and Sharman, R. D.: Combined winds and turbulence prediction system for automated air-traffic management applications, J. Appl. Meteorol. Clim., 54, 766–784, doi:10.1175/JAMC-D-14-0216.1, 2015. 11819

Koch, S. E., Jamison, B. D., Lu, C., Smith, T. L., Tollerud, E. I., Girz, C., Wang, N., Lane, T. P., Shapiro, M. A., Parrish, D. D., and Cooper, O. R.: Turbulence and gravity waves within an upper-level front, J. Atmos. Sci., 62, 3885–3908, doi:10.1175/JAS3574.1, 2005. 11819

Lester, P.: Turbulence – A New Perspective for Pilots, Jeppesen Sanderson, Engelwood, CO, USA, 1994. 11818, 11833

Monin, A. S. and Yaglom, A. M.: Statistical Fluid Mechanics, vol. 2, MIT Press, Cambridge, MA, USA, 1975. 11827

NASA: U.S. Standard Atmosphere, National Aeronautics and Space Administration, Washington, USA, available at: http://ntrs.nasa.gov/archive/nasa/casi.ntrs.nasa.gov/19770009539.pdf (last access: 13 August 2015), 1976. 11829

NTSB: Review of U.S. Civil Aviation Accidents 2007–2009, Tech. Rep. NTSB/ARA-11/01, National Transportation Safety Board, Washington, USA, available at: www.ntsb.gov/investigations/data/Documents/ARA1101.pdf (last access: 6 August 2015), 2011. 11818

NTSB: Review of U.S. Civil Aviation Accidents 2010, Tech. Rep. NTSB/ARA-12/01, National Transportation Safety Board, available at: www.ntsb.gov/investigations/data/Documents/ARA1201.pdf (last access: 6 August 2015), 2012. 11818

AMTD

8, 11817–11852, 2015

Clear-air turbulence information from regular commercial aircraft

J. M. Kopeć et al.

Poggi, D. and Katul, G. G.: Evaluation of the turbulent kinetic energy inside canopies by zero- and level-crossing density methods, Bound.-Lay. Meteorol., 136, 219–233, doi:10.1007/s10546-010-9503-2, 2010. 11828, 11829, 11831, 11833

Sharman, R., Tebaldi, C., Wiener, G., and Wolff, J.: An integrated approach to mid- and upper-level turbulence forecasting, Weather Forecast., 21, 268–287, doi:10.1175/WAF924.1, 2006. 11819

Sharman, R. D., Trier, S. B., Lane, T. P., and Doyle, J. D.: Sources and dynamics of turbulence in the upper troposphere and lower stratosphere: a review, Geophys. Res. Lett., 39, L12803, doi:10.1029/2012GL051996, 2012. 11819

Sharman, R. D., Cornman, L. B., Meymaris, G., Pearson, J., and Farrar, T.: Description and derived climatologies of automated in situ eddy-dissipation-rate reports of atmospheric turbulence, J. Appl. Meteorol. Clim., 53, 1416–1432, doi:10.1175/JAMC-D-13-0329.1, 2014. 11831

Sreenivasan, K. R.: On the universality of the Kolmogorov constant, Phys. Fluids, 7, 2778–2784, doi:10.1063/1.868656, 1995. 11828, 11831

Trier, S. and Sharman, R. D.: Convection-permitting simulations of the environment supporting widespread turbulence within the upper-level outflow of a mesoscale convective system, Mon. Weather Rev., 137, 1972–1990, 2009. 11819

Trier, S., Sharman, R. D., Fovell, R. G., and Frehlich, R. G.: Numerical simulation of radial cloud bands within the upper-level outflow of an observed mesoscale convective system, J. Atmos. Sci., 67, 2990–2999, 2010. 11818, 11819

Trier, S. B., Sharman, R. D., and Lane, T. P.: Influences of moist convection on a cold-season outbreak of Clear-Air Turbulence (CAT), Mon. Weather Rev., 140, 2477–2496, doi:10.1175/MWR-D-11-00353.1, 2012. 11818

Veerman, H., Vrancken, P., and Lombard, L.: Flight testing delicat – a promise for medium-range clear air turbulence protection, in: European 46th SETP and 25th SFTE Symposium, Luleå, Sweden, 15–18 June 2014, available at: https://hal.archives-ouvertes.fr/hal-01111380 (last access: 7 August 2015), 2014. 11819, 11821

Vrancken, P.: Airborne remote detection of turbulence with forward-looking LIDAR, in: Aviation Turbulence – Processes, Detection, Prediction, edited by: Sharman, R. D. and Lane, T. P., Springer, Cham, Switzerland, 2015. 11819

Williams, J.: Using random forests to diagnose aviation turbulence, Mach. Learn., 95, 51–70, doi:10.1007/s10994-013-5346-7, 2014. 11819

AMTD
8, 11817–11852, 2015

WMO: Aircraft Meteorological Data Relay (AMDAR) Reference Manual, World Meteorological Organization, WMO-No. 958, Geneva, Switzerland, 2003. 11822, 11825, 11827, 11832
Wright, J. R. and Cooper, J. E.: Introduction to Aircraft Aeroelasticity and Loads, John Wiley and Sons, Chichester, UK, 2014. 11827

AMTD
8, 11817–11852, 2015

Clear-air turbulence information from regular commercial aircraft

J. M. Kopeć et al.

Table 1. Parameters and basic characteristics of the KNMI data used in this paper. Nominal reporting frequency is based on whether the parameter is ADS-B or Mode-S EHS content. Data availability is a percent of all aircraft reports where the parameter was successfully received and decoded.

Data type	Data resolution	Nominal sample rate	Data availability
Longitude	0.00024°	> 1 Hz	100.0 %
Latitude	0.00002°	> 1 Hz	100.0 %
Ground speed	2 kt (1.03 $m s^{-1}$)	> 1 Hz	5.6 %
True Airspeed	2 kt (1.03 $m s^{-1}$)	0.2 Hz	5.6 %
Altitude	25 ft (7.62 m)	> 1 Hz	99.6 %
Vertical rate	64 $ft min^{-1}$ (0.32 $m s^{-1}$)	> 1 Hz	99.7 %
Heading	0.1757°	0.2 Hz	52.1 %

AMTD
8, 11817–11852, 2015

Clear-air turbulence information from regular commercial aircraft

J. M. Kopeć et al.

Table 2. Parameters of DELICAT data used in this paper and their respective data sources.

Data type	Data source	Sample rate
Longitude	IRS	5 Hz
Latitude	IRS	5 Hz
True airspeed	DADC	8 Hz
Baro Corrected Altitude	DADC	16 Hz
Vertical rate	DADC	16 Hz
Track Angle	IRS	20 Hz
Ground speed	IRS	10 Hz
Heading	IRS	20 Hz

AMTD
8, 11817–11852, 2015

Table 3. Summary of the EDR estimation approaches.

Method	Performance	Advantages	Disadvantages
ADS-B EDR	– IVV EDR: Mostly satisfactory but very significant false positives found – ALT EDR: Significant noise, only FL9 MOD identified	– Global coverage – Only one free parameter	– Aircraft type dependent – Performance issues (both ALT EDR and IVV EDR).
Mode-S Structure Function EDR	Very good	– Potentially aircraft independent – Only one free parameter	– Coverage limited by SSR range
Mode-S Threshold Crossing EDR	Good, some small issues in FL6	– Potentially aircraft independent	– Coverage limited by SSR range – 3 free parameters

AMTD
8, 11817–11852, 2015

AMTD
8, 11817–11852, 2015

Clear-air turbulence information from regular commercial aircraft

J. M. Kopeć et al.

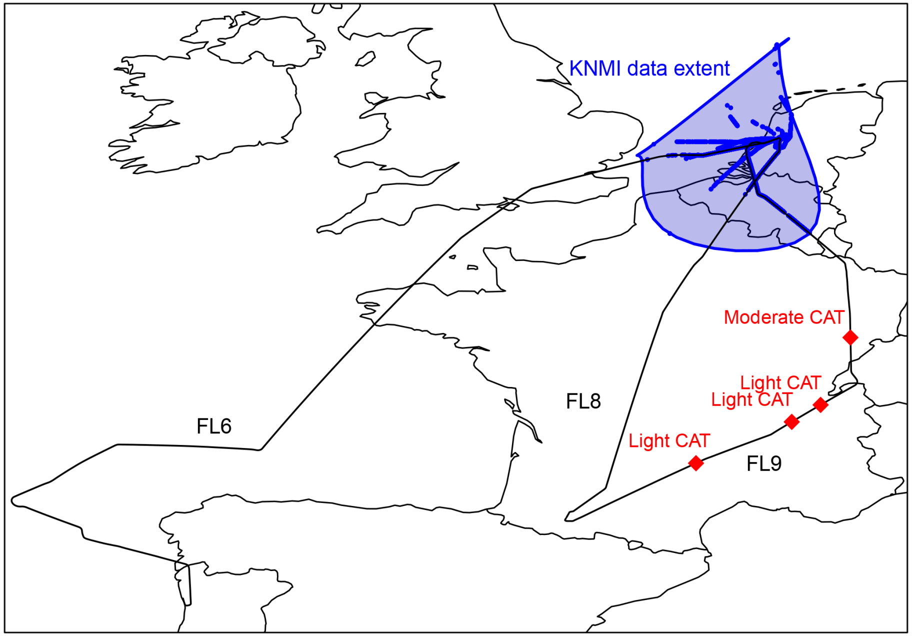

Figure 1. Tracks of DELICAT flights FL6, FL8 and FL9 (black solid lines). Peak turbulent events (red markers and red caption). KNMI data (blue dots) and KNMI data range (light blue shape).

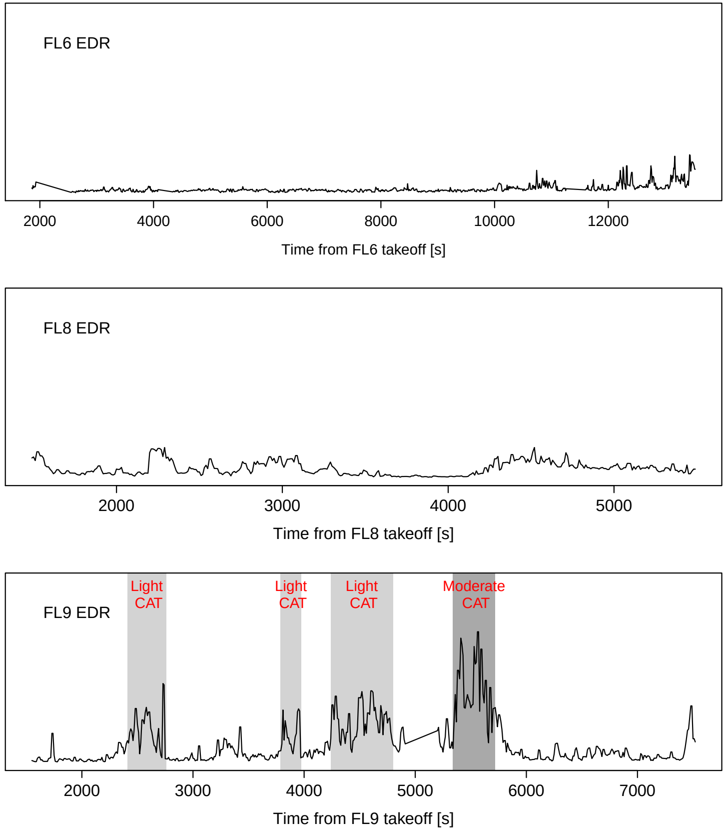

Figure 2. Reference EDR recordings from the DELICAT flights FL6, FL8 and FL9. Plots show 15 s maxima of the EDR in the cruise fragments of the flights. Vertical scale is arbitrary (yet the same on all plots) as EDR is scalable by a constant. Shaded areas in FL9 pane are the CAT occurrences (as in Fig. 1).

AMTD
8, 11817–11852, 2015

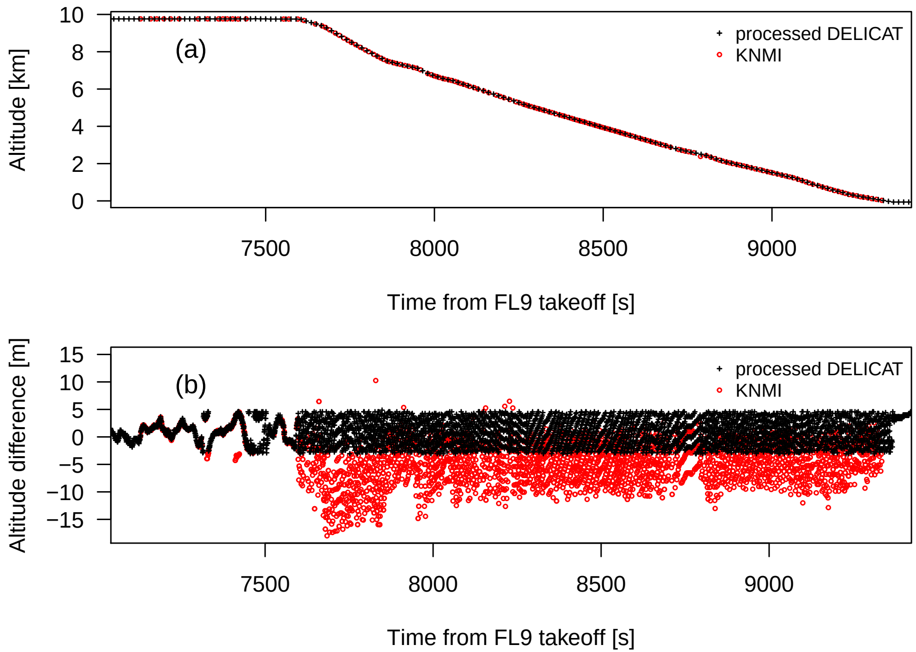

Figure 3. A comparison between the processed DELICAT data (black crosses) and KNMI data (red circles) of **(a)** the altitude profile (note that for the sake of clearness 97 % of the observations are not plotted here) and **(b)** the difference of the altitude with respect to the DELICAT reference altitude.

AMTD
8, 11817–11852, 2015

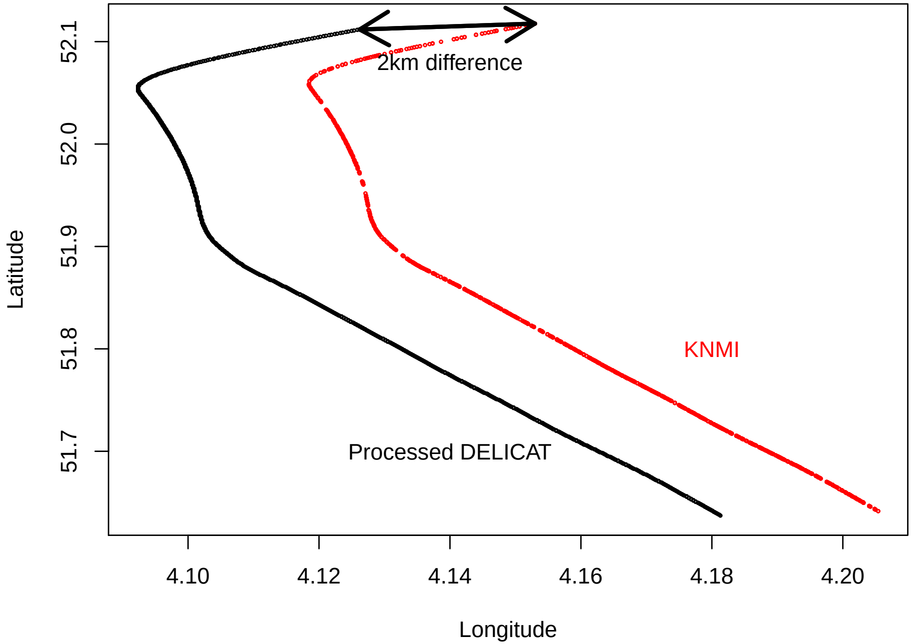

Figure 4. Comparison of flight paths as recorded by the KNMI receiver (red dots) and resulting from the processing of the DELICAT data (black dots) for a fragment of FL9. The 2 km error can be attributed to IRS drift which is of the order of 3 km per hour. IRS was calibrated prior to each flight.

AMTD
8, 11817–11852, 2015

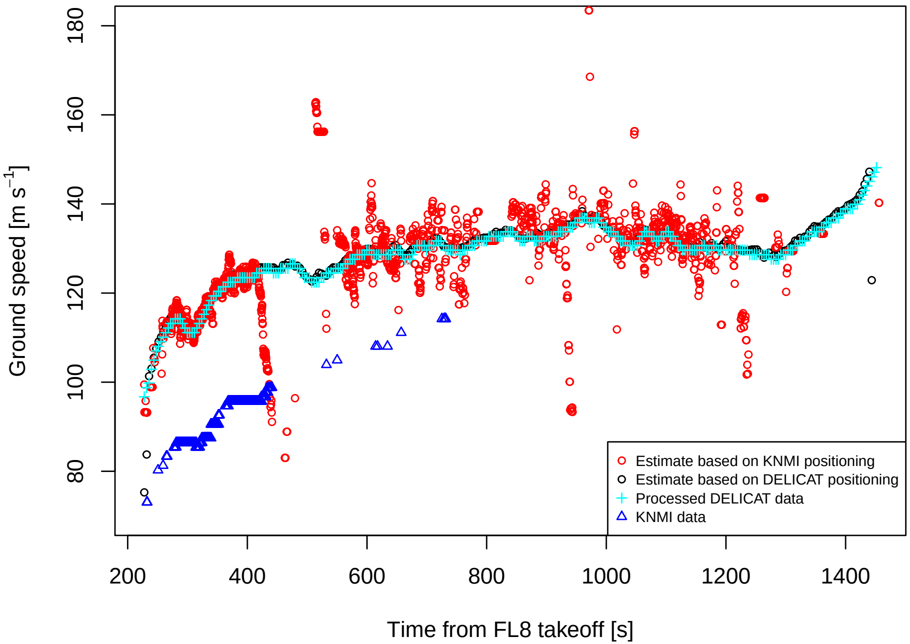

Figure 5. Comparison of ground speed record against estimates based on reported geographic position for the case of FL8. FL8 is presented because of the longest continuous KNMI record containing ground speed.

AMTD
8, 11817–11852, 2015

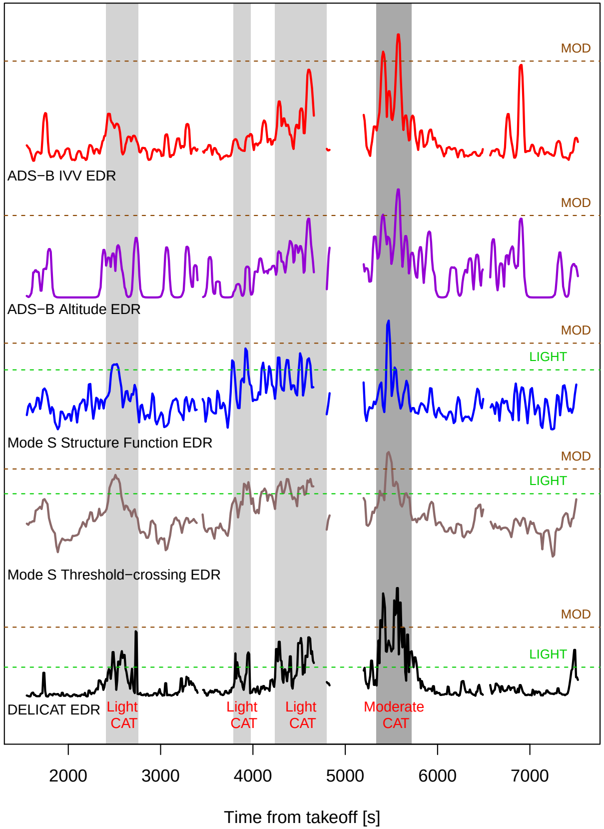

Figure 6. Results for FL9 for all analysed approaches to estimate EDR and a reference EDR (as in Fig. 2). The time series are scaled to match the intensity of the MOD event. For reference the tentative turbulence levels have been added to the plot. Those are reflecting the FL9 encounters and levels of noise inferred from the calm flights.

AMTD
8, 11817–11852, 2015

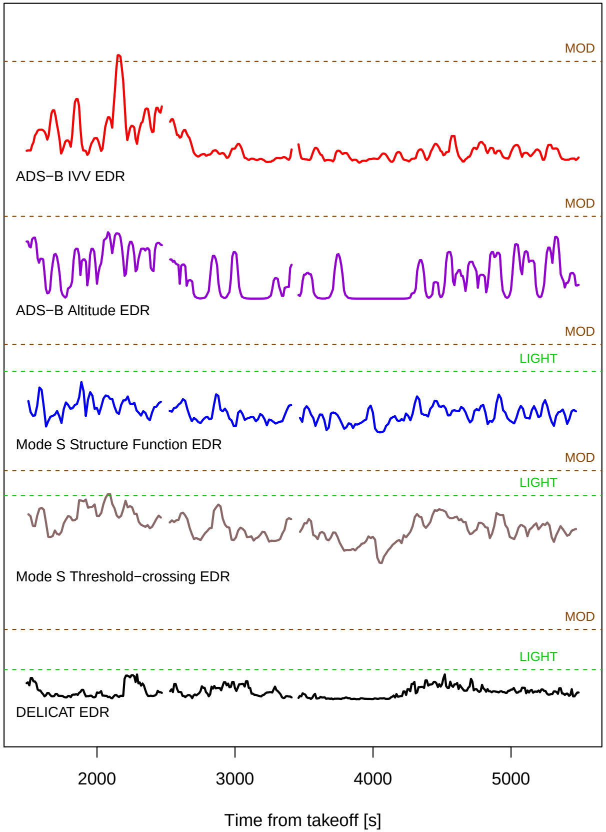

Figure 7. Results for FL8 for all analysed approaches to estimate EDR and a reference EDR (as in Fig. 2). The time series are scaled to match the intensity of the FL9 MOD event. For reference the tentative turbulence levels have been added to the plot. Those are reflecting the FL9 encounters and levels of noise inferred from the calm flights.

AMTD
8, 11817–11852, 2015

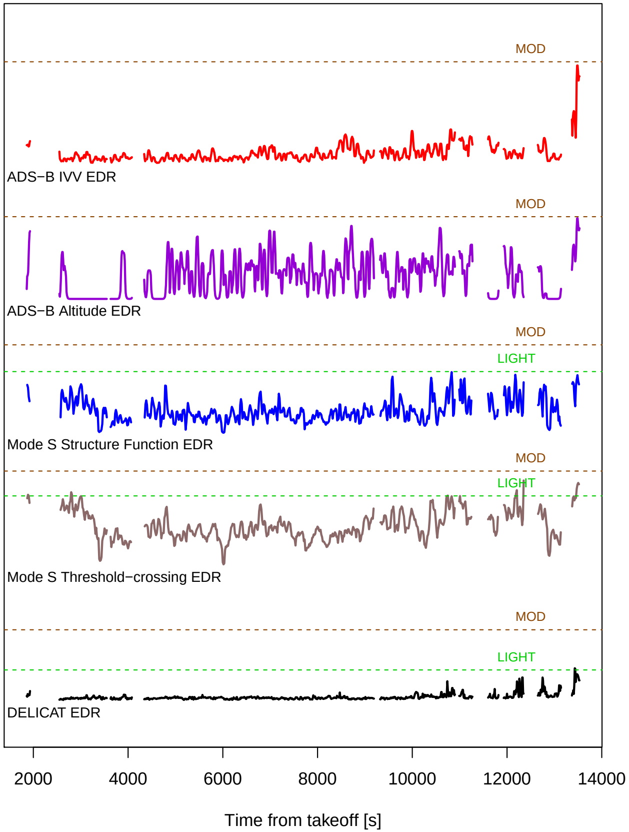

Figure 8. Results for FL6 for all analysed approaches to estimate EDR and a reference EDR (as in Fig. 2). The time series are scaled to match the intensity of the FL9 MOD event. For reference the tentative turbulence levels have been added to the plot. Those are reflecting the FL9 encounters and levels of noise inferred from the calm flights.

AMTD
8, 11817–11852, 2015

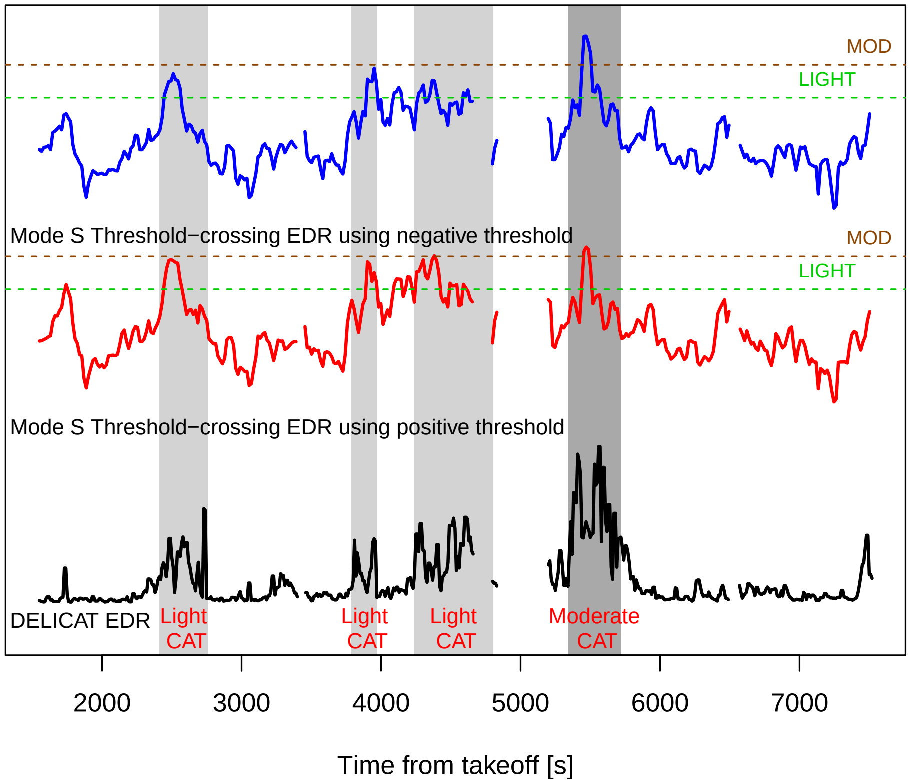

Figure 9. Comparison of the threshold-crossing method results for $T_C = 0.4$ for positive and negative threshold.

AMTD
8, 11817–11852, 2015

Clear-air turbulence information from regular commercial aircraft

J. M. Kopeć et al.

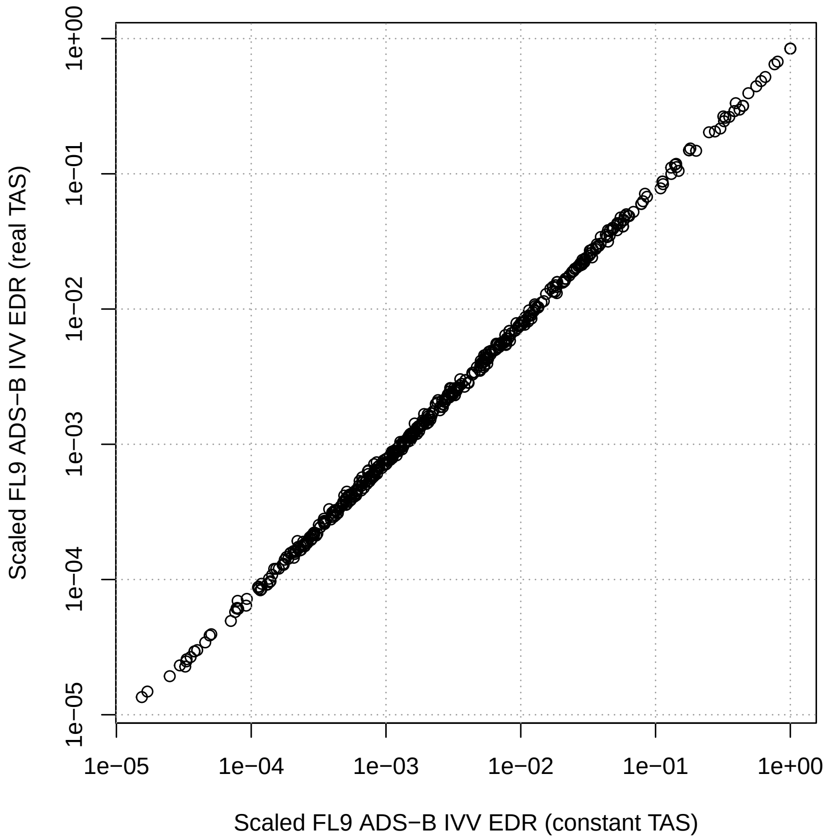

Figure 10. An exemplary comparison of EDR for FL9 calculated using IVV method using the real TAS record vs. the constant TAS approximation. We used $250\,\mathrm{m\,s^{-1}}$ as the constant TAS. Both of the EDR estimates were scaled to the range of values of constant TAS EDR thus are unitless and in approximate range 0–1.

AMTD
8, 11817–11852, 2015

Clear-air turbulence information from regular commercial aircraft

J. M. Kopeć et al.